

## DISCLAIMER

This report was prepared as an account of work sponsored by an agency of the United States Government. Neither the United States Government nor any agency thereof, nor any of their employees, makes any warranty, express or implied, or assumes any legal liability or responsibility for the accuracy, completeness, or usefulness of any information, apparatus, product, or process disclosed, or represents that its use would not infringe privately owned rights. Reference herein to any specific commercial product, process, or service by trade name, trademark, manufacturer, or otherwise does not necessarily constitute or imply its endorsement, recommendation, or favoring by the United States Government or any agency thereof. The views and opinions of authors expressed herein do not necessarily state or reflect those of the United States Government or any agency thereof.

# Computer-Aided Methods of Determining Thyristor Thermal Transients

E. Lu and G. Bronner

Princeton Plasma Physics Laboratory  
Princeton, New Jersey 08543

PPPL--2548

DE88 015826

### Abstract

An accurate tracing of the thyristor thermal response is investigated. This paper offers several alternatives for thermal modeling and analysis by using an electrical circuit analog: topological method, convolution integral method, etc. These methods are adaptable to numerical solutions and well suited to the use of the digital computer.

The thermal analysis of thyristors was performed for the 1000 MVA converter system at the Princeton Plasma Physics Laboratory. Transient thermal impedance curves for individual thyristors in a given cooling arrangement were known from measurements and from manufacturer's data. The analysis pertains to almost any loading case, and the results are obtained in a numerical or a graphical format.

**MASTER**

DISTRIBUTION OF THIS DOCUMENT IS UNLIMITED

CP

## 1 Introduction

In all electrical equipment temperature rise has an important effect on equipment rating. A thyristor is no exception. Any property of a thyristor is temperature-dependent, and the maximum allowable junction temperature is one factor that determines its rating. In order to provide the junction with sufficient thermal reserve (the temperature rise margin), it is necessary to assess correctly the temperature and transient temperature changes for normal and anomalous loading situations.

Thermal conditions for a thyristor are typically calculated from power dissipation, taking into consideration the possible load cycle, the current waveforms, and the cooling conditions. The total power losses,  $P_{tot}$ , of a thyristor are the sum of the on-state losses, switching losses (losses during turning on and turning off the device), gate power losses, off-state losses, and reverse losses [1]. At industrial frequencies between 0 and 400 c.p.s., the on-state dissipation dominates the heating of the junction [2]. The other losses, within the margin of error, can be neglected. For any current waveform, the instantaneous on-state dissipation equals the product of ~~peak~~ on-state current and voltages. In Fig. 1 an on-state characteristic of a thyristor is shown. The instantaneous on-state voltage under consideration can be expressed as  $v = r_F i + V_{T0}$  [1]. Thus,

$$\begin{aligned} p &= vi \\ &= V_{T0}i + r_F i^2, \end{aligned}$$

where

$$\begin{aligned} V_{T0} &= \text{threshold voltage} \\ r_F &= \text{forward resistance.} \end{aligned}$$

A portion of the heat is conducted through the casing and heat sink. The amount of heat conducted depends on the thermal resistance. The rest of the heat increases the device temperature. Thus, the junction temperature is a function of the dissipation as well as of the thermal resistances and capacitances.

In steady-state operation, after thermal equilibrium has set in, the heat flow rate and the temperature distribution in the system are constant. The released heat passes through a number of components

made of different materials and geometries. Thermally, these parts can be modeled using their thermal resistances connected in series [3]. Figure 2 shows the thermal equivalent circuit of a steady-state, where the heat is assumed to be dissipated at one point of the junction.  $\theta$ ,  $P$ , and  $R$  indicate temperature, power dissipation, and thermal resistance, respectively, and the subscripts  $j$ ,  $c$ ,  $s$ , and  $a$  denote junction, casing, heat sink and ambient, respectively. The junction temperature rise above ambient temperature is

$$\theta_j = P(R_{jc} + R_{cs} + R_{sa}).$$

In normal operation a thyristor is supplied from a conventional 60 Hz power system, so the conduction period,  $\tau$ , is a fraction of  $1/60 = 0.0167$  seconds. In a three-phase (6 pulse) bridge circuit, the pulse lasts one-third of a cycle (120 electrical degrees). The conduction period is  $0.0167 \times 120/360 = 5.6 \times 10^{-3}$  seconds as shown in part B of Fig. 3<sup>1</sup>. The time dependence of the power loss is similar to that of the current. Hence, during the load cycle the device experiences several heating and cooling periods.

The similarity between the heat flow and Ohm's Law is conducive to the idea of finding analogies between heat transfer and the conduction of electricity. The concept of thermal resistance anticipates the concept of a thermal circuit as an analog to the electric circuit. A transient thermal impedance  $Z_{th}(t)$ , which approaches the thermal resistance  $R_{th}$  at  $t \rightarrow \infty$ , can be employed to determine the maximum junction temperature in the pulsed operation.  $Z_{th}$  is defined as the change in temperature between two specified points or regions in response to the step function change in power dissipation [4]. The value is affected by the thermal capacitances as well as by the thermal resistances of the device. If the time dependence of the transient thermal impedance of a thyristor (mounted on a given heat sink in a given cooling arrangement) is known, then the junction temperature  $\theta_j$  is given at any arbitrary instant.

The analytic treatments of transient heat conditions for a thyristor are generally rather formidable. Satisfactory approximate solutions, however, can be obtained using numerical methods suitable for digital

<sup>1</sup>This approximation assumes zero-time for commutation.

computers. In this paper, we present solutions which are based on an electrical analog with a *network synthesis* and *analysis* technique. In the analog model, power dissipation corresponds to current and temperature to voltage.

## 2 Network Synthesis

*Synthesis* is defined as the realization of passive networks that satisfy the given transfer functions. A solution may not exist if the given function is not realizable. A check should be made to determine whether the given function satisfies the *necessary and sufficient* conditions for physical realization.

In our synthesis application, the thermal impedance specification is given in a graphical form, i.e., transient thermal impedance curves for individual thyristors in a given cooling arrangement. In this case, before a network realization can be initiated, the given curve must be approximated by an appropriate rational function, using a certain *curve fitting* method. After the rational function has been determined, there is no further approximation: realization of the rational function by a network is exact.

### 2.1 Approximation – Curve Fitting

In *curve fitting* we are given  $n$  points

$$(x_1, y_1), \dots, (x_n, y_n)$$

and we want to determine a function  $f(x)$  such that

$$f(x_j) \approx y_j, \quad j = 1, \dots, n$$

Figure 4 shows a typical transient thermal impedance curve (junction-to-water) with exponential characteristics that allow a series of decay exponential functions to be found. Our approach to *curve fitting* is to use successive regression in semilogarithmic space. A step-by-step procedure is as follows:

1. Sample a set of data points  $\{t_i, Z_{tht}(t_i)\}$  from the given transient thermal impedance curve.
2. To start with, choose a set of new data points  $\{t_i, y(t_i)\}$ , where  $y(t_i) = R_{th} - Z_{tht}(t_i)$  and  $R_{th}$  is the steady-state thermal impedance.
3. Graph the selected points on semilogarithmic scales and fit them with piecewise straight lines, satisfying  $\max \left\{ \frac{g(t_i) - y(t_i)}{g(t_i)} \right\} < \epsilon$ , where  $\{t_i, g(t_i)\}$  is the point lying on the line.
4. Define a difference function for the  $j_{th}$ -time segment,

$$\delta_j(t) = g(t) - f_{j-1}(t) \quad (j = 1, n - 1), \quad (1)$$

where  $f_{j-1}(t)$  is the analytic term for the  $(j + 1)_{th}$ -time segment corresponding to the  $(j - 1)_{th}$ -straight line and  $n$  is the total number of straight lines.

5. Initiate the *fitting* calculation from the right side to the left side in the coordinate :

- The equation for the  $n_{th}$ -time segment,

$$\ln f_n(t) = -\alpha_n t + \ln C_n.$$

By taking an antilogarithm on both sides,

$$f_n(t) = C_n e^{-\alpha_n t},$$

where

$$\begin{cases} \alpha_n = \ln \frac{g(t_{n,1})}{g(t_{n,2})} / (t_{n,2} - t_{n,1}) \\ C_n = g(t_{n,1}) e^{\alpha_n t_{n,1}}. \end{cases}$$

The subscripts 1 and 2 denote two distinctive points on the  $n_{th}$ -straight line. The same is true for the following.

- The equation for the  $(n - 1)_{th}$ -time segment,

$$\ln \delta_{n-1}(t) = -\alpha_{n-1} t + \ln C_{n-1}.$$

By taking an antilogarithm on both sides,

$$\delta_{n-1}(t) = C_{n-1} e^{-\alpha_{n-1} t},$$

where

$$\begin{cases} \alpha_{n-1} = \ln \frac{\delta_{n-1}(t_{n-1,1})}{\delta_{n-1}(t_{n-1,2})} / (t_{n-1,2} - t_{n-1,1}) \\ C_{n-1} = \delta_{n-1}(t_{n-1,1}) e^{\alpha_{n-1} t_{n-1,1}} \end{cases}$$

Guided by Eq. (1), we determine:

$$\begin{aligned} f_{n-1}(t) &= f_n(t) + \delta_{n-1}(t) \\ &= C_n e^{-\alpha_n t} + C_{n-1} e^{-\alpha_{n-1} t} \end{aligned}$$

• In general, we have

$$\begin{aligned} \delta_{n-i}(t) &= g(t) - f_{n-i+1}(t) \\ &= C_{n-i} e^{-\alpha_{n-i} t} \quad (i = 1, n-1), \end{aligned}$$

where

$$\begin{cases} \alpha_{n-i} = \ln \frac{\delta_{n-i}(t_{n-i,1})}{\delta_{n-i}(t_{n-i,2})} / (t_{n-i,2} - t_{n-i,1}) \\ C_{n-i} = \delta_{n-i}(t_{n-i,1}) e^{\alpha_{n-i} t_{n-i,1}} \end{cases}$$

Thus,

$$\begin{aligned} f_{n-i}(t) &= f_{n-i+1}(t) + \delta_{n-i}(t) \\ &= C_n e^{-\alpha_n t} + \dots + C_{n-i} e^{-\alpha_{n-i} t} \quad (i = 1, n-1), \end{aligned}$$

in terms of the definition,  $\delta_{n-i}(t)$  nearly drops down to the zero when approaching the end of the  $(n-i)_{th}$ -time interval, and  $f_{n-i}(t) \approx g(i)$  thenceforth.

6. Following  $(n-1)$ -steps operations we can represent  $Z_{tht}(t)$ , referring to (2):

$$\begin{aligned} Z_{tht}(t) &= R_{th} - f_1(t) \\ &= R_{th} - C_n e^{-\alpha_n t} - \dots - C_1 e^{-\alpha_1 t} \\ &= R_{th} - \sum_{i=1}^n C_i e^{-\alpha_i t} \end{aligned} \quad (2)$$

The above procedure can be easily implemented in a computer program. A flow chart used to determine the *curve fitting* coefficients  $C_i$  &  $\alpha_i$ , ( $i=1..n$ ) is shown in the Appendix. Based on the series fitting that is given in Fig. 5, a close agreement with the original thermal impedance curve is clearly evident, where  $n = 5$  was chosen.

## 2.2 Network Realization

To transform the transient thermal impedance  $Z_{tht}(t)$  from a time domain (Eq.2) to an analog circuit takes two steps:

- Find the system function of Eq.(2) with respect to a unit-step excitation.
- Convert the system function into an RC network, which is suggested by the nature of the thermal problem.

A driving-point function  $G$  of the system shown in Fig. 6, may be derived from the definition of the transient thermal impedance and Eq. (2):

$$\begin{aligned}
 G(s) &= \frac{\mathcal{L}\{Z_{tht}(t)\}}{\mathcal{L}\{p(t)\}} \\
 &= \frac{Z_{tht}(s)}{P(s)} \\
 &= \left( \frac{R_{th}}{s} - \sum_{i=1}^n \frac{C_i}{s + \alpha_i} \right) / \frac{1}{s} \\
 &= \left( R_{th} - \sum_{i=1}^n C_i \right) + \sum_{i=1}^n \frac{C_i \alpha_i}{s + \alpha_i} \\
 &= k_0 + \sum_{i=1}^n \frac{k_i}{s + \alpha_i}, \tag{3}
 \end{aligned}$$

where  $k_0 = R_{th} - \sum_{i=1}^n C_i$ ,  $k_i = C_i \alpha_i$ . The function  $G(s)$  satisfies the *necessary* and *sufficient* conditions for physical realization [5].

Through a sequence of mathematical operations with multiplication and addition of polynomials, the system function  $G$  shown in Eq.(3) can be transcribed to a rational-fraction of two polynomials





Thus, the product of matrices  $\vec{C} \times \vec{Q}$  is a  $(m+n-1) \times 1$  matrix which contains the coefficients of the product  $F(s) = P(s) \times Q(s)$ . A listing of subroutine **PMUL** which will perform such an operation is given in the Appendix.

The procedures for combining groups of two fractions in Eq.(3) were developed with matrix multiplication and addition arithmetic. Instead of a detailed description of the operation, several steps to find the coefficients of the numerator and denominator polynomials are demonstrated as follows:

$$\frac{k_1}{s + \alpha_1} + \frac{k_2}{s + \alpha_2} = \frac{k_1(s + \alpha_2) + k_2(s + \alpha_1)}{(s + \alpha_1)(s + \alpha_2)} = \frac{(k_1 + k_2)s + (k_1\alpha_2 + k_2\alpha_1)}{s^2 + (\alpha_1 + \alpha_2)s + \alpha_1\alpha_2}$$

The above step in matrix arithmetic will read :

For the numerator,

$$\begin{bmatrix} k_1 & 0 \\ 0 & k_2 \end{bmatrix} \begin{bmatrix} 1 \\ \alpha_2 \end{bmatrix} + \begin{bmatrix} k_2 & 0 \\ 0 & k_1 \end{bmatrix} \begin{bmatrix} 1 \\ \alpha_1 \end{bmatrix} = \begin{bmatrix} k_1 + k_2 \\ k_1\alpha_2 + k_2\alpha_1 \end{bmatrix},$$

i.e., the top row has the coefficient of  $s^1$ , the second row has  $s^0$ . In general, the  $i_{th}$ -row contains the coefficient of  $s^{ndeg-i+1}$ , where  $ndeg$  is the degree of the product polynomial.

For the denominator,

$$\begin{bmatrix} 1 & 0 \\ \alpha_1 & 1 \\ 0 & \alpha_1 \end{bmatrix} \begin{bmatrix} 1 \\ \alpha_2 \end{bmatrix} = \begin{bmatrix} 1 \\ \alpha_1 + \alpha_2 \\ \alpha_1\alpha_2 \end{bmatrix},$$

i.e., the top row has the coefficient of  $s^2$ , etc. and continue with

$$\frac{(k_1 + k_2)s + (k_1\alpha_2 + k_2\alpha_1)}{s^2 + (\alpha_1 + \alpha_2)s + \alpha_1\alpha_2} + \frac{k_3}{s + \alpha_3} = \dots$$

for numerator,

$$\begin{bmatrix} k_1 - k_2 & 0 \\ k_1\alpha_2 - k_2\alpha_1 & k_1 - k_2 \\ 0 & k_1\alpha_2 + k_2\alpha_1 \end{bmatrix} \begin{bmatrix} 1 \\ \alpha_3 \end{bmatrix} + \begin{bmatrix} k_3 & 0 & 0 \\ 0 & k_3 & 0 \\ 0 & 0 & k_3 \end{bmatrix} \begin{bmatrix} 1 \\ \alpha_1 + \alpha_2 \\ \alpha_1\alpha_2 \end{bmatrix} \\ = \begin{bmatrix} k_1 + k_2 - k_3 \\ k_1(\alpha_2 + \alpha_3) + k_2(\alpha_1 + \alpha_3) + k_3(\alpha_1 + \alpha_2) \\ k_1\alpha_2\alpha_3 - k_2\alpha_1\alpha_3 + k_3\alpha_1\alpha_2 \end{bmatrix}.$$

for denominator,

$$\begin{bmatrix} 1 & 0 \\ \alpha_1 - \alpha_2 & 1 \\ \alpha_1 \alpha_2 & \alpha_1 - \alpha_2 \\ 0 & \alpha_1 \alpha_2 \end{bmatrix} \begin{bmatrix} 1 \\ \alpha_3 \end{bmatrix} = \begin{bmatrix} 1 \\ \alpha_1 - \alpha_2 - \alpha_3 \\ \alpha_1 \alpha_2 + \alpha_1 \alpha_3 + \alpha_2 \alpha_3 \\ \alpha_1 \alpha_2 \alpha_3 \end{bmatrix}$$

The algorithm may be easily designed by calling the subroutine **PMUL** to collect the appropriate terms for powers of  $s$ .

The rational fraction as shown in Eq.(4), in turn, can be manipulated to define an RC ladder with resistances in the series arms and capacitances in the shunt arms alternately where the values of R and C are determined by the steps of a *continued-fraction expansion* [5]. The first step of such a process may be shown as follows, assuming  $G(0) > G(\infty)$  and  $b_0 \neq 0$  [5]:

$$\frac{b_n s^n + b_{n-1} s^{n-1} + \dots}{a_n s^n + a_{n-1} s^{n-1} + \dots} \left[ \frac{z_1}{a_n/b_n} \right]$$

$$\frac{\frac{a_n}{b_n} b_{n-1} s^{n-1} + \dots}{a_{n-1} - \frac{a_n}{b_n} b_{n-1}} s^{n-1} + \dots$$

$$\underbrace{\hspace{10em}}_{a'_{n-1}}$$

Thus, from the first step, we obtain a result of the form,

$$G(s) = \frac{A(s)}{B(s)} = \frac{a_n}{b_n} + \frac{1}{\frac{b_n s^n + b_{n-1} s^{n-1} + \dots}{a'_{n-1} s^{n-1} + a'_{n-2} s^{n-2} + \dots}}$$

where  $a'_{n-1} = [a_{n-1} - \frac{a_n}{b_n} b_{n-1}]$ , etc. The next step is

$$\frac{a'_{n-1} s^{n-1} + a'_{n-2} s^{n-2} + \dots}{b_n s^n + b_{n-1} s^{n-1} + \dots} \left[ \frac{z_2}{(b_n/a'_{n-1})s} \right]$$

$$\frac{\frac{b_n}{a'_{n-1}} a'_{n-2} s^{n-1} + \dots}{[b_{n-1} - \frac{b_n}{a'_{n-1}} a'_{n-2}] s^{n-1} + \dots}$$

$$\underbrace{\hspace{10em}}_{b'_{n-1}}$$

Up to the second step, we may write the function in the form,

$$C'(s) = \frac{a_n}{b_n} - \frac{1}{\frac{b_{n-1}}{a_{n-1}}s + \frac{1}{\frac{a'_{n-1}s^{n-1} - a'_{n-2}s^{n-2} + \dots}{b'_{n-1}s^{n-1} - b'_{n-2}s^{n-2} + \dots}}}$$

where  $b'_{n-1} = b_{n-1} - \frac{b_n}{a_{n-1}}a'_{n-2}$ , etc.

The repetition of the basic two-step procedure for cycles will continue to give partial quotients that are alternately positive constants and linear terms with positive coefficients until the number of partial quotients obtained in the continued-fraction expansion is equal to one more than the number of internal critical frequencies, which are the zeros and poles collectively [5]. The algorithm is easily implemented by a subroutine **CFE** which is listed in the Appendix.

Figure 6 shows the schematic representation of the ladder network corresponding to this expansion on the basis of the transient thermal impedance curve shown in Fig. 4 with resistance terminations at both input and output. The series arms are labeled with their impedance values  $z$  and the shunt arms with their admittance values (capacitances)  $y$ . There is a value of thermal resistance assigned to each group of resistors in series. The first group identified is the internal thermal resistance from junction to case, given in the individual device specifications. Next is the sum of the contact thermal resistance from the case to the heat exchanger and the thermal resistance of the heat exchanger to the cooling medium, of which value is the difference between two steady-state thermal impedances as shown in Fig. 4.

### 3 Transient Thermal Analysis

The previous model was developed to perform the thermal analysis. A solution always exists and is unique where an input is given. There are several methods to solve the thermal problem which are equivalent to solving the transient behavior of an electrical circuit.

### 3.1 Classical and State-Variable Methods

A part of synthesis - network realization - bears directly on the *classical* and *state-variable* methods and provides considerable insight into thermal equivalent circuit operation, which allows the temperature distribution in the thermal system to be found.

The dynamics of an RC circuit are determined by the rate of change of the capacitor voltages in the circuit. The first-order ordinary differential equations describing the circuit should be established in terms of the topology of the circuit, and solved by numerical means due to discontinuous loading cases in converter bridges. Both *classical* and *state-variable* methods present such a scheme in obtaining the time-domain response of networks to arbitrary inputs. The detailed contents and computer algorithms may be found in standard texts and are omitted here.

### 3.2 Convolution Integral Method

If we are interested only in the response on thyristor junctions, then numerical solution of the convolution integral method should be used. The advantage over the other methods is to omit the lengthy network realization process mentioned in the previous section and rely on the system function defined in Eq.(3). This will be elaborated below.

Assume a network's response to an impulse input  $\delta(t)$  is known  $h(t)$ , then, for an arbitrary input  $p(t)$ , the *convolution integral* will find the response  $\theta_j(t)$  [6]:

$$\begin{aligned}\theta_j(t) &= \int_0^t p(t-\tau)h(\tau)d\tau \\ &= \int_0^t p(\tau)h(t-\tau)d\tau \\ &= p(t) * h(t) \quad (t \geq 0).\end{aligned}$$

The integral applies only to linear, time-invariant networks and requires only that  $p(t)$  and  $h(t)$  be Laplace transformable. The situation is illustrated in Fig.7. In the upper figure, we introduce an impulse to the zero-state network G at  $t=0$  and obtain the output response

$h(t)$ . Now if we apply some other function  $p(t)$  at  $t=0$  to the same network  $G$ , we obtain the response  $\theta_j(t) = p(t) * h(t)$ . In Fig. 7 the network is a black box, and  $G(s)$  is defined by input-output relations in accordance with Eq. (3). The inverse Laplace transform of the system function  $G(s)$  shows that the impulse response includes terms of the form  $k_i e^{-\alpha_i t}$ , where  $k_i$  is a constant and  $\alpha_i$  is the zero of the denominator polynomial. From Eq. (3),

$$\begin{aligned} h(t) &= \mathcal{L}^{-1}\{G(s)\} \\ &= k_0 \delta(t) + \sum_{i=1}^n k_i e^{-\alpha_i t}. \end{aligned}$$

Thus, to arbitrary input  $p(t)$ :

$$\begin{aligned} \theta_j(t) &= p(t) * h(t) \\ &= p(t) * [k_0 \delta(t) + \sum_{i=1}^n k_i e^{-\alpha_i t}] \\ &= k_0 p(t) * \delta(t) + \sum_{i=1}^n k_i [p(t) * e^{-\alpha_i t}] \\ &= k_0 p(t) + \sum_{i=1}^n k_i \int_0^t p(\tau) e^{-\alpha_i(t-\tau)} d\tau \\ &= k_0 p(t) + \sum_{i=1}^n k_i e^{-\alpha_i t} \underbrace{\int_0^t p(\tau) e^{\alpha_i \tau} d\tau}_{J_i(t)} \quad (t \geq 0). \end{aligned}$$

We noted that the response of a dynamic network depends on *present* and *past* events. The partial solution, i.e. the value of integration  $J_i(t) = \int_0^t p(\tau) e^{\alpha_i \tau} d\tau$ , may be obtained analytically in a few simple cases, such as  $p(t) = c$  or  $p(t) = kt + c$ . For varying loading requirements a numerical method of approximate integration should be used when analytical solutions are difficult to obtain. The results are accurate only within some tolerance, depending on the program and the basic machine characteristics.

For a certain loading cycle as shown in part *A* of Fig. 3 and a current through an individual thyrister in part *B*, a *trapezoidal integration algorithm* may be adopted. The flowchart for the logic of such

a numerical algorithm to find the thyristor thermal response is presented in the Appendix. The computer algorithm advances by taking finite steps in the independent variable  $t$ . During pulsed-operation a suitably small increment is clearly required for accuracy. For the sake of economy, values of integration in which the algorithm is equipped to recognize jump discontinuities, once calculated, are saved as the *memory* of past events for the next step. The flowchart may help to explain the performance. The response obtained using the algorithm, corresponding to the loading case with reference to Fig. 3, is sketched in Fig. 9.

## 4 Conclusions

Methods to analyze the transient thermal response of a thyristor were developed. An improved knowledge of the junction temperature excursion can result in better protection and significant savings for pulsed loads or transient loading conditions. An important preliminary finding indicates significant junction cooling in milliseconds of the *off* periods. The continuous current operation is considered as the special case of the discontinuous current operation to which this analysis is dedicated.

## Acknowledgments

The authors would like to thank the Engineering Analysis Division for support during the course of this work, and also thank L. Ku who helped in developing the *curve fitting* technique. The work was sponsored by the U. S. Dept. of Energy Contract No. DE-AC02-76-CHO-3073.

## References

- [1] Thorborg, K., *Power Electronics*, 2nd Ed., S. T. Teknik, Sweden, 1985, pp.2:1-2:18.
- [2] Csáki, F., Ganszky, K., Ipsits, I. and Marti, S., *Power Electronics*, Akadémiai Kiadó, Budapest, 1975, p.567.
- [3] Sugandhi, R. K. and Sugandhi, K. K., *Thyristors Theory and Applications*, 2nd Ed., John Wiley & Sons, Inc., New York, 1984, pp.25-35.
- [4] The Engineering Staff of International Rectifier, *SCR Applications Handbook*, International Rectifier Corp., El Segundo, 1974, p.476.
- [5] Weinberg, L., *Network Analysis and Synthesis*, McGraw-Hill Book Company, Inc., New York, 1962.
- [6] Jensen, R. W. and Watkins, B. O., *Network Analysis Theory and Computer Methods*, Prentice-Hall, Inc., Englewood Cliffs, 1974, pp.307-313.





## A Listing for the Subroutine PMUL

```

c      subroutine pmul(p,m,q,n,f,mn)
c      Subroutine for performing multiplication of polynomials  $f(s)=p(s)q(s)$ .
c      Arguments m - degree of polynomial p(s). (input)
c      p - array of length m+1 containing the coefficients
c      of polynomial p(s). (input)
c      n - degree of polynomial q(s). (input)
c      q - array of length n+1 containing the coefficients
c      of polynomial q(s). (input)
c      mn - m+n degree of product polynomial f(s). (input)
c      f - output array of length mn+1 containing the
c      coefficients of product polynomial f(s).
c      dimension p(0:m),q(0:n),f(0:mn)
c
c      Initiate the coefficients of the f array to zero.
c      do 1 i=0,mn
c      f(i)=0.
1     continue
c
c      Compute the coefficients of terms with powers i (i=0,mn).
c      do 3 i=0,mn
c      do 2 j=0,i
c      f(mn-i)=p(m-i+j)q(n-j)+f(mn-i)
c      Test to make certain that maximum number of terms
c      to the above summation is n+1 if m > n.
c      if(j.eq.n) go to 3
2     continue
3     continue
c
c      Compute the coefficients of terms with power i (i=0,n-1).
c      do 5 i=n-1,0,-1
c      do 4 j=0,i
c      f(i)=p(j)q(i-j)+f(i)
c      Test to make certain that maximum number of terms
c      to the above summation is m+1 if m < n.
c      if(j.eq.m) go to 5
4     continue
5     continue
c      return
c      end

```

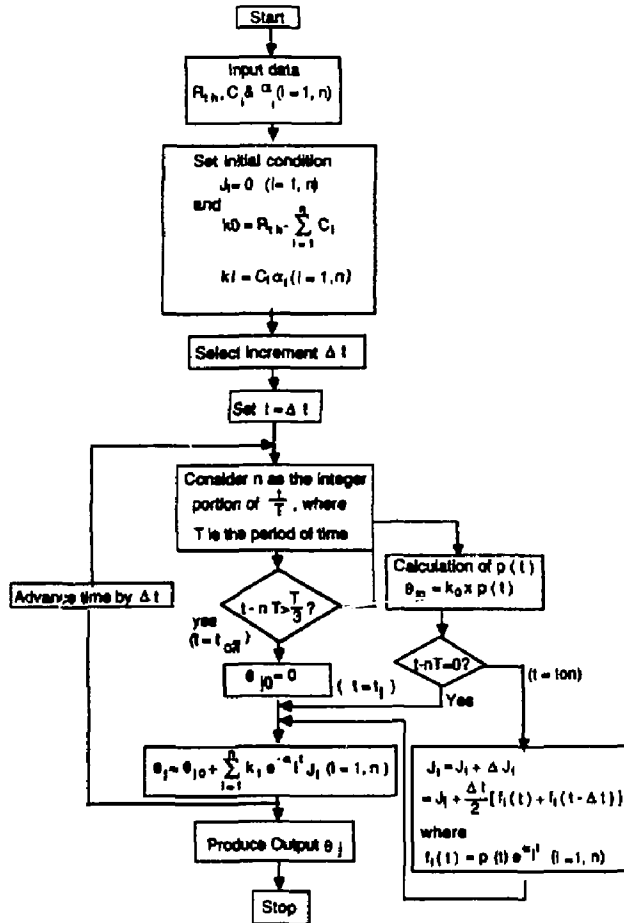
## A Listing for the Subroutine CFE

```

      subroutine cfe(a,b,n,c,ip,np)
c     Subroutine for performing continued-fraction expansion
c     about infinity for a rational fraction of equal degrees
c     in numerator and denominator.
c     Arguments  n - degree of polynomials.(input)
c               a - array of coefficients of numerator polynomial.(input)
c               b - array of coefficients of denominator polynomial.(input)
c               np - number of partial quotients.(output)
c               c - output array of coefficients of partial quotients.
c               ip - output array of powers of partial quotients.
c               dimension a(0:n),b(0:n),c(2n+1),ip(2n+1)
c               data eps /.1e-8 /
c
c     Perform the continued-fraction expansion procedure np (≤ 2n+1) times.
      np=2n+1
      m=n
      k=0
c     The first operation of the basic two-step procedure in C.F.E. :
10    j=2*k+1
c     Compute the coefficients and powers of partial quotients.
      c(j)=a(n)/b(n)
      ip(j)=m-n
      if(j.eq.np) go to 100
c     Find a new remainder polynomial of degree mdeg
c     as a new denominator of the second operation.
      mdeg=0
      do 20 i=1,n
        a(m-1)=a(m-i)-c(j)*b(n-i)
        if((a(m-1).gt.eps).and.(mdeg.eq.0)) mdeg=m-i
20    continue
      if(mdeg.ne.(m-1)) np=np-(m-1-mdeg)
      m=mdeg
c
c     The second operation of the basic two-step procedure in C.F.E. :
      j=2*(k+1)
c     Compute the coefficients and powers of partial quotients.
      c(j)=b(n)/a(m)
      ip(j)=n-m
      if(j.eq.np) go to 100
c     Find a new remainder polynomial of degree ndeg
c     as a new denominator of the following cycle.
      ndeg=0
      do 30 i=1,m
        b(n-1)=b(n-i)-c(j)*a(m-i)
        if((b(n-1).gt.eps).and.(ndeg.eq.0)) ndeg=n-i
30    continue
      if(ndeg.ne.(n-1)) np=np-(n-1-ndeg)
      n=ndeg
c
      k=k+1
      go to 10
100  return
      end

```

A Flow Chart for Finding Response by Trapezoidal Algorithm †



† with reference to Fig. 8

## Figure Captions

**Fig. 1** Forward drop curve for currents, showing an on-state characteristic of a thyristor

**Fig. 2** Thermal model of a thyristor in steady-state operations.

**Fig. 3** TFTR loading curves. Part *B* represents the current through individual thyristors in a three-phase (6 pulse) bridge circuit, supplied from a conventional 60 Hz power system.

**Fig. 4** Transient thermal impedance curve for individual thyristors in a given cooling arrangement from measurements and manufacturer's data.

**Fig. 5** Transient thermal impedance *fitting* curve by approximation.

**Fig. 6** Thermal model of the thyristor corresponding to Fig. 4, where

$$\begin{aligned} Z_{tht}(t) &= R_{th} - \sum_{i=1}^5 C_i e^{-\alpha_i t} \\ &= 0.07 - 0.04899e^{-0.03892t} - 0.009827e^{-0.4274t} - \\ &\quad 0.003508e^{-1.964t} - 0.00453e^{-11.02t} - 0.002049e^{-183.3t} \\ &\quad (\text{°C/W}) \end{aligned}$$

and

$$G(s) = \frac{0.001096s^5 + 0.6541s^4 - 19.60s^3 - 67.66s^2 + 47.46s + 4.620}{s^5 + 196.8s^4 + 2493.s^3 + 5089.s^2 + 1881.s - 65.99}$$

**Fig. 7** Illustration of Convolution.

**Fig. 8** Geometrical interpretation of a definite integral having a pulsed-integrand with jump discontinuities. As shown in the figure,  $t_{on}$ ,  $t_{off}$ , and  $t_l$  indicate time during *on* period, *off* period, and *leading* edge, respectively.  $T$  is the period of time.

**Fig. 9** Thyristor thermal response curves, carried out on the transient thermal impedance curve in Fig. 4 and the loading case with reference to Fig. 3. Part *B* shows the enlargement of a small interval. It is obvious that the temperature rise and fall curves follow the well-known exponential law, where jump discontinuities are caused by the assumption of zero-time commutation.

#88E0025

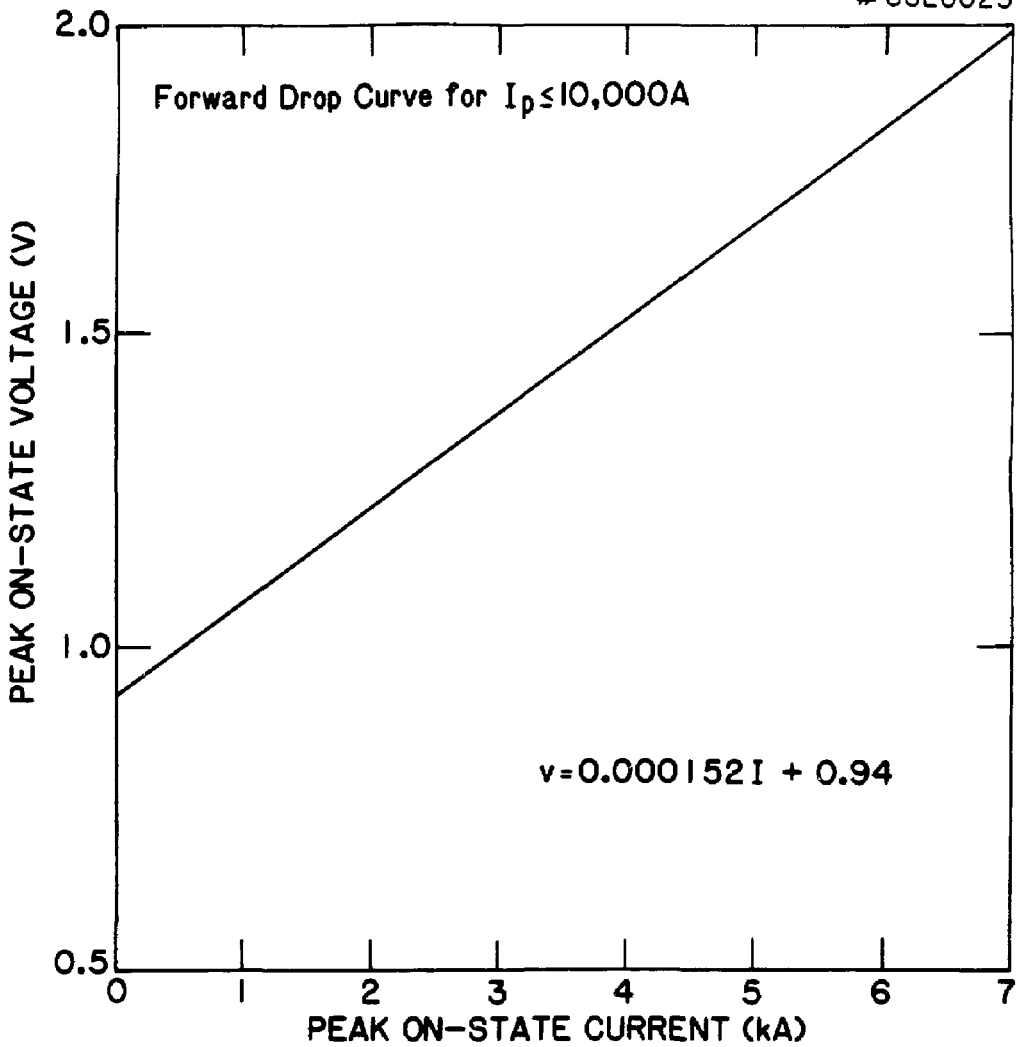


Fig. 1

## THERMAL MODEL OF A THYRISTOR IN STEADY-STATE OPERATION

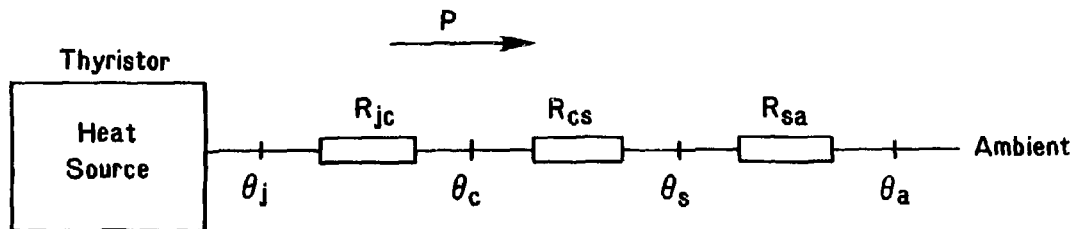


Fig. 2

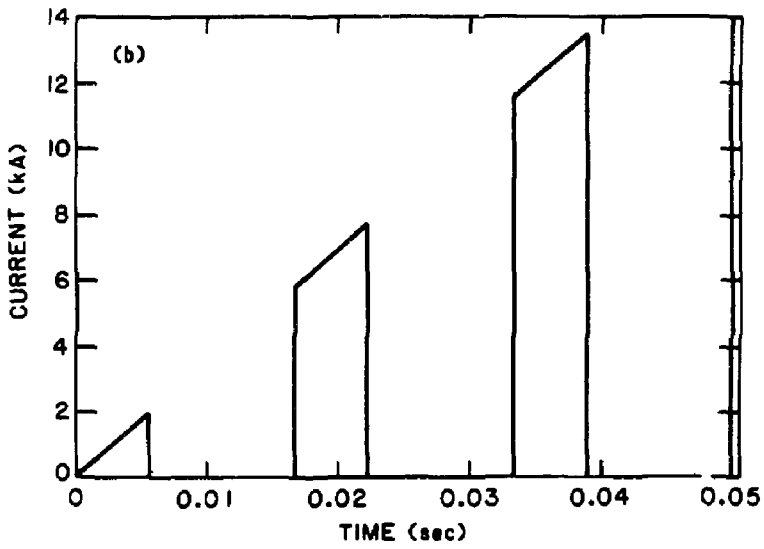
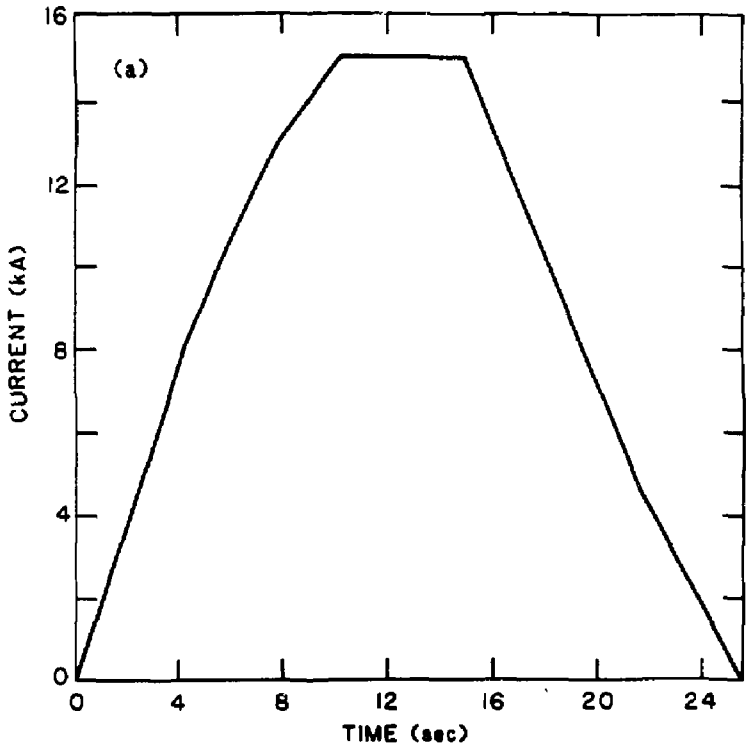
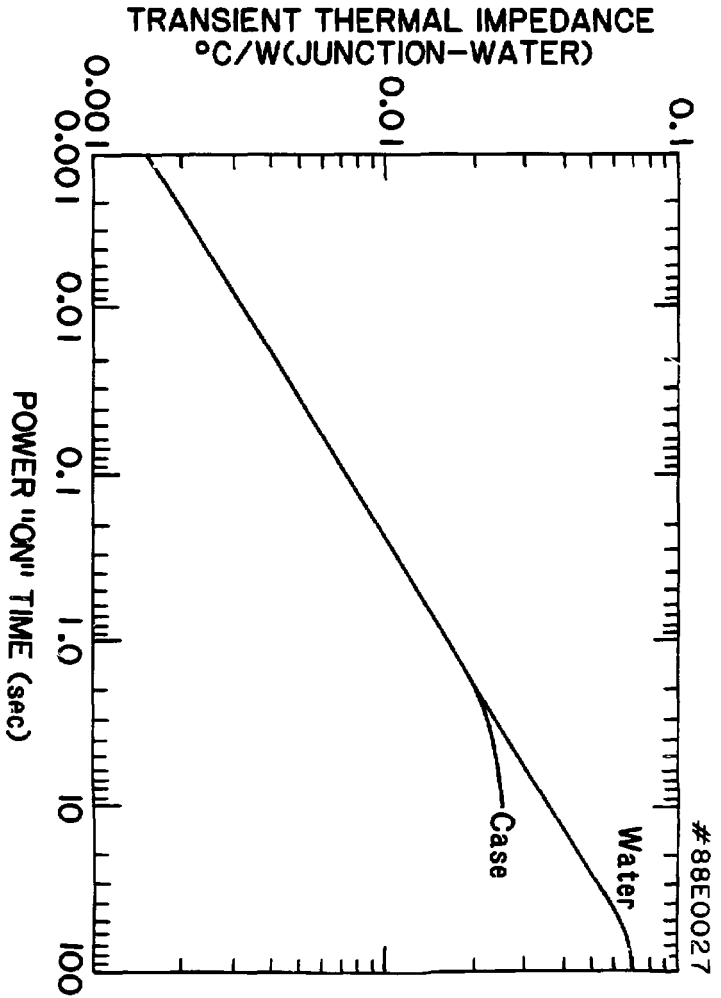


Fig. 3

Fig. 4





#88E0026

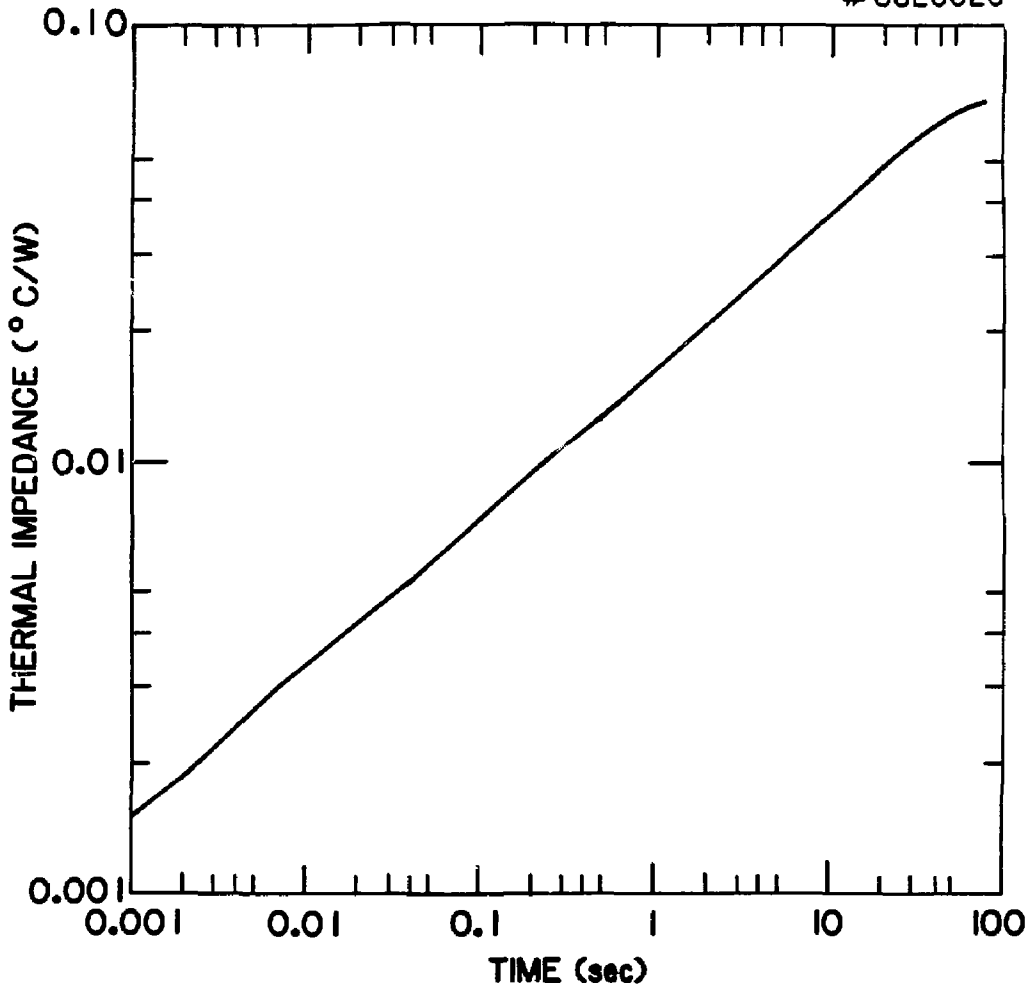


Fig. 6

## THERMAL MODEL OF THYRISTOR

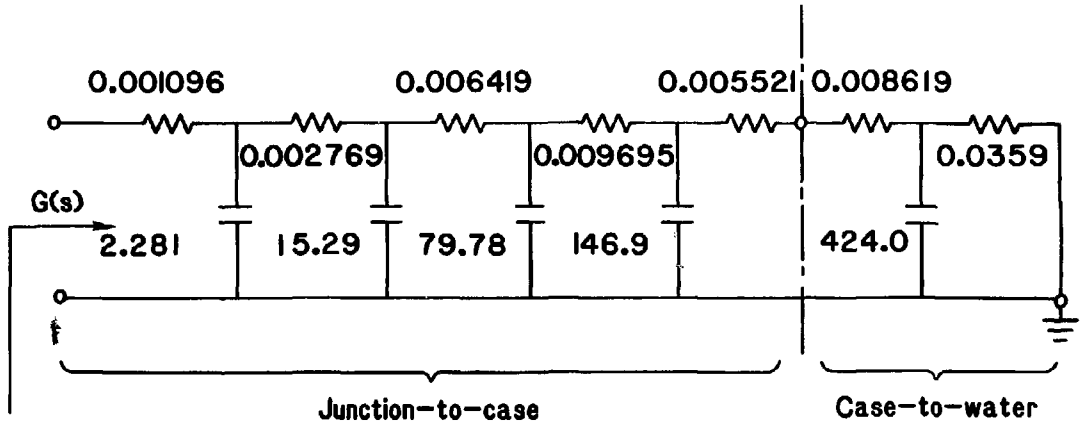


Fig. 5

# ILLUSTRATION OF CONVOLUTION

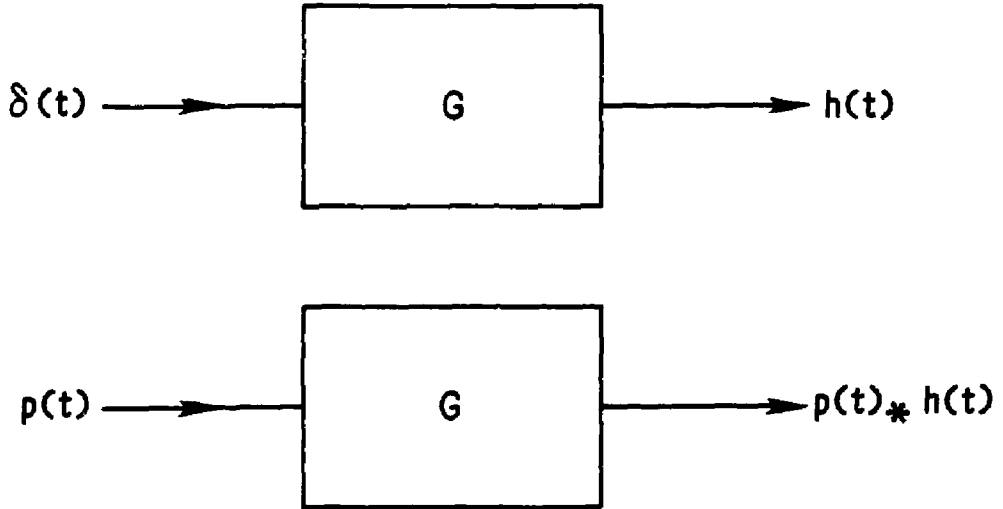


Fig. 7

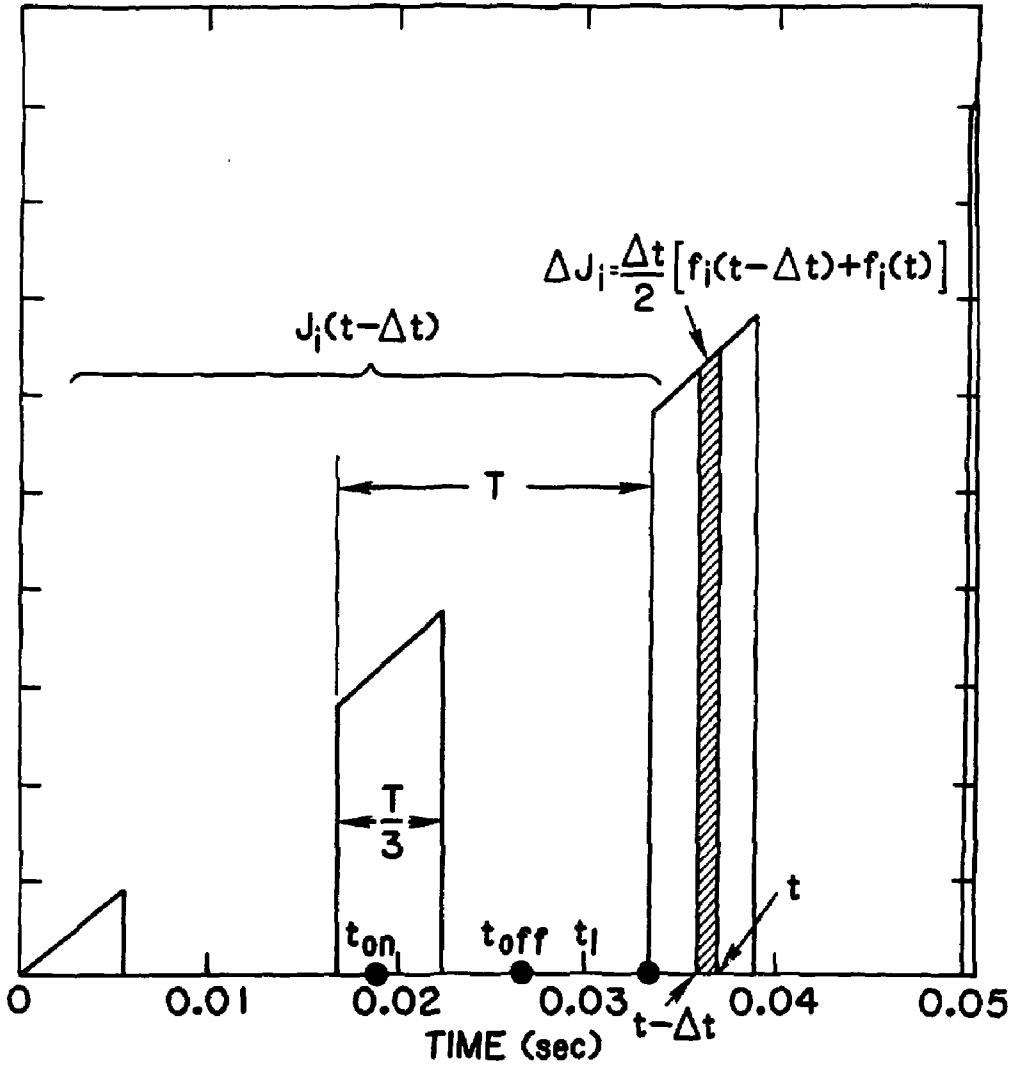


Fig. 8

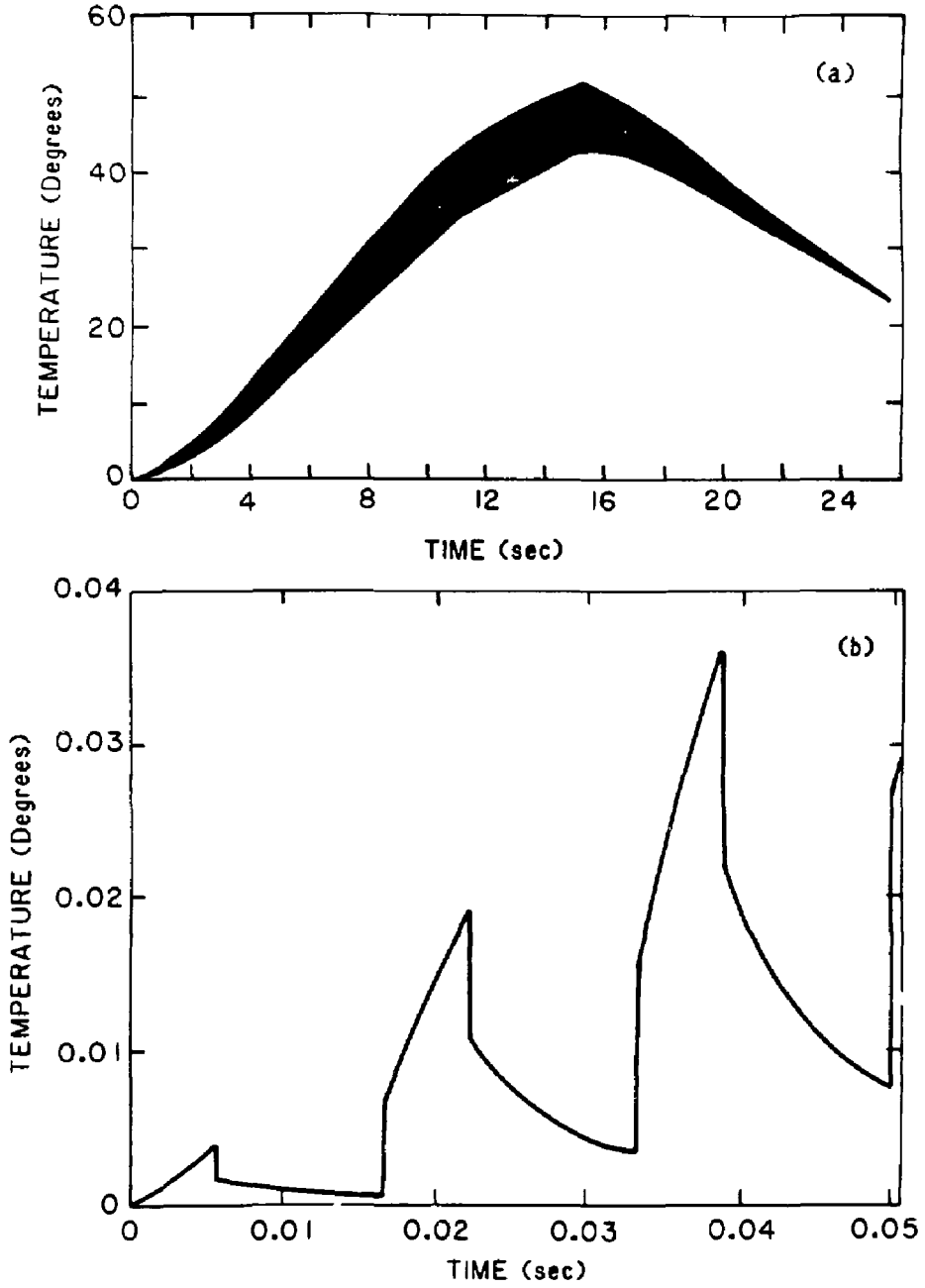


Fig. 9

EXTERNAL DISTRIBUTION IN ADDITION TO UC-20

Dr. Frank J. Paoloni, Univ of Wollongong, AUSTRALIA  
Prof. M.H. Brennan, Univ Sydney, AUSTRALIA  
Plasma Research Lab., Australian Nat. Univ., AUSTRALIA  
Prof. I.R. Jones, Flinders Univ., AUSTRALIA  
Prof. F. Cap, Inst Theo Phys, AUSTRIA  
Prof. M. Heindler, Institut für Theoretische Physik, AUSTRIA  
M. Goossens, Astronomisch Instituut, BELGIUM  
Ecole Royale Militaire, Lab de Phys Plasmas, BELGIUM  
Commission-European, Dg-XII Fusion Prog, BELGIUM  
Prof. R. Boucique, Laboratorium voor Natuurkunde, BELGIUM  
Dr. P.H. Sakonaka, Instituto Fisica, BRAZIL  
Instituto De Pesquisas Espaciais-INPE, BRAZIL  
Documents Office, Atomic Energy of Canada Limited, CANADA  
Dr. M.P. Bachynski, MPB Technologies, Inc., CANADA  
Dr. H.M. Skarsgard, University of Saskatchewan, CANADA  
Dr. H. Bernard, University of British Columbia, CANADA  
Prof. J. Teichmann, Univ. of Montreal, CANADA  
Prof. S.R. Sreenivasan, University of Calgary, CANADA  
Prof. Tudor W. Johnston, INRS-Energie, CANADA  
Dr. C.R. James, Univ. of Alberta, CANADA  
Dr. Peter Lukac, Komenského Univ, CZECHOSLOVAKIA  
The Librarian, Culham Laboratory, ENGLAND  
The Librarian, Rutherford Appleton Laboratory, ENGLAND  
Mrs. S.A. Hutchinson, JET Library, ENGLAND  
C. Mouttet, Lab. de Physique des Milieux Ionisés, FRANCE  
J. Radet, CEN/CADARACHE - Bat 506, FRANCE  
Univ. of Ioannina, Library of Physics Dept. GREECE  
Dr. Tom Mui, Academy Bibliographic Ser., HONG KONG  
Preprint Library, Hungarian Academy of Sciences, HUNGARY  
Dr. B. Dasgupta, Saha Inst of Nucl. Phys., INDIA  
Dr. P. Kaw, Institute for Plasma Research, INDIA  
Dr. Philip Rosenau, Israel Inst. Tech, ISRAEL  
Librarian, Int'l Ctr Theo Phys, ITALY  
Prof. G. Rostagni, Univ Di Padova, ITALY  
Miss Clelia De Palo, Assoc EURATOM-ENEA, ITALY  
Biblioteca, Instituto di Fisica del Plasma, ITALY  
Dr. H. Yamato, Toshiba Res & Dev, JAPAN  
Prof. I. Kawakami, Atomic Energy Res. Institute, JAPAN  
Prof. Kyoji Nishikawa, Univ of Hiroshima, JAPAN  
Direc. Dept. Large Tokamak Res. JAERI, JAPAN  
Prof. Satoshi Itoh, Kyushu University, JAPAN  
Research Info Center, Nagoya University, JAPAN  
Prof. S. Tanaka, Kyoto University, JAPAN  
Library, Kyoto University, JAPAN  
Prof. Nobuyuki Inoue, University of Tokyo, JAPAN  
S. Mori, JAERI, JAPAN  
Librarian, Korea Advanced Energy Res. Institute, KOREA  
Prof. D.I. Choi, Adv. Inst Sci & Tech, KOREA  
Prof. B.S. Liley, University of Waikato, NEW ZEALAND  
Institute of Plasma Physics, PEOPLE'S REPUBLIC OF CHINA  
Librarian, Institute of Phys., PEOPLE'S REPUBLIC OF CHINA  
Library, Tsing Hua University, PEOPLE'S REPUBLIC OF CHINA  
Z. Li, Southwest Inst. Physics, PEOPLE'S REPUBLIC OF CHINA  
Prof. J.A.C. Cabral, Inst Superior Tecnico, PORTUGAL  
Dr. Octavian Petrus, AL I CUZA University, ROMANIA  
Dr. Johan de Villiers, Fusion Studies, AEC, SO AFRICA  
Prof. M.A. Hellberg, University of Natal, SO AFRICA  
C.I.E.M.A.T., Fusion Div. Library, SPAIN  
Dr. Lennart Stenflo, University of UMEA, SWEDEN  
Library, Royal Inst Tech, SWEDEN  
Prof. Hans Wilhelmson, Chalmers Univ Tech, SWEDEN  
Centre Phys des Plasmas, Ecole Polytech Fed, SWITZERLAND  
Bibliotheek, Fom-Inst voor Plasma-Fysica, THE NETHERLANDS  
Dr. D.D. Ryutov, Siberian Acad Sci, USSR  
Dr. G.A. Eliseev, Kurchatov Institute, USSR  
Dr. V.A. Glukhikh, Inst Electrophysical Apparatus, USSR  
Dr. V.T. Tolok, Inst. Phys. Tech. USSR  
Dr. L.M. Kovrizhnykh, Institute Gen. Physics, USSR  
Nuclear Res. Establishment, Julich Ltd., W. GERMANY  
Bibliothek, Inst. für Plasmaforschung, W. GERMANY  
Dr. K. Schindler, Ruhr Universität Bochum, W. GERMANY  
ASDEX Reading Rm, IPP/Max-Planck-Institut für  
Plasmaphysik, W. GERMANY  
Librarian, Max-Planck Institut, W. GERMANY  
Prof. R.K. Janev, Inst Phys, YUGOSLAVIA